Journal of Inflammation Research

Dovepress
open access to scientific and medical research

Open Access Full Text Article

ORIGINAL RESEARCH

RETRACTED ARTICLE: Synthesis, In Silico and Pharmacological Evaluation of New Thiazolidine-4-Carboxylic Acid Derivatives Against Ethanol-Induced Neurodegeneration and Memory Impairment

Shagufta Naz[1,2], Lina Tariq Al Kury[3], Humaira Nadeem[1], Fawad Ali Shah[1], Aman Ullah[1], Rehan Zafar Paracha[4], Muhammad Imran[5], Shupeng Li[2]

[1]Riphah Institute of Pharmaceutical Sciences, Riphah International University, Islamabad, 44000, Pakistan; [2]State Key Laboratory of Oncogenomics, School of Chemical Biology and Biotechnology, Shenzhen Graduate School, Peking University, Shenzhen, People's Republic of China; [3]College of Natural and Health Sciences, Zayed University, Abu Dhabi, 49153, United Arab Emirates; [4]Research Center for Modeling & Simulation (RCMS), National University of Sciences and Technology (NUST), Islamabad, 44000, Pakistan; [5]Department of Pharmacy, IQRA University, Islamabad, 44000, Pakistan

Correspondence: Humaira Nadeem, Riphah Institute of Pharmaceutical Sciences, Riphah International University, Islamabad, 44000, Pakistan, Tel +92 51-2891835, Fax +92 51-8350180, Email humaira.nadeem@riphah.edu.pk; Shupeng Li, State Key Laboratory of Oncogenomics, School of Chemical Biology and Biotechnology, Shenzhen Graduate School, Peking University, Shenzhen, People's Republic of China, Email lisp@pku.edu.cn

Introduction: Several studies revealed that alcohol utilization impairs memory in adults; however, the underlying mechanism is still unclear. The production of inflammatory markers and reactive oxygen species (ROS) plays a major role in neurodegeneration, which leads to memory impairment. Therefore, targeting neuroinflammation and oxidative distress could be a useful strategy for abrogating the hallmarks of ethanol-induced neurodegeneration. Moreover, several studies have demonstrated multiple biological activities of thiazolidine derivatives including neuroprotection.

Methods: In the current study, we synthesized ten (10) new thiazolidine-4-carboxylic acid derivatives (P1-P10), characterized their synthetic properties using proton nuclear magnetic resonance (¹H-NMR) and carbon-13 NMR, and further investigated the neuroprotective potential of these compounds in an ethanol-induced neuroinflammation model.

Results: Our results suggested alterations levels of antioxidant enzymes associated with an elevated level of tumor necrosis factor-alpha (TNF-α), nuclear factor-κB (p-NF-κB), pyrin domain-containing protein 3 (NLRP3), and cyclooxygenase-2 (COX-2) in ethanol-treated animals. Ethanol treatment also led to memory impairment in rats, as assessed by behavioral tests. To further support our notion, we performed molecular docking studies, and all synthetic compounds exhibited a good binding affinity with a fair bond formation with selected targets (NF-κB, TLR4, NLRP3, and COX-2).

Discussion: Overall, our results revealed that these derivatives may be beneficial in reducing neuroinflammation by acting on different stages of inflammation. Moreover, P8 and P9 treatment attenuated the neuroinflammation, oxidative stress, and memory impairment that caused by ethanol.

Keywords: thiazolidine, oxidative stress, neuroinflammation, neuroprotective, molecular docking, ethanol

Introduction

Neurodegenerative diseases (NDs) represent a greater hazard to humans, more precisely to the elderly population,[1] and it will surpass cancer in the next 20 years according to WHO.[2] These diseases encompass multiple neurological disorders characterized by diverse arrays of pathophysiologies and accompanied either by cognitive impairments and/or disability in movements among others.[3] It includes a range of disorders, with the two most common being Alzheimer's and Parkinson's disease.[4] Another exacerbating factor is the progressive accumulation and dysfunctional trafficking of misfolded proteins in the brain such as amyloid-beta (Aβ) and tau protein in the case of Alzheimer's disease.[5] Neurodegenerative diseases share many fundamental processes associated with neuronal dysfunction and death such as

Received: 5 January 2022
Accepted: 4 June 2022
Published: 25 June 2022

Graphical Abstract

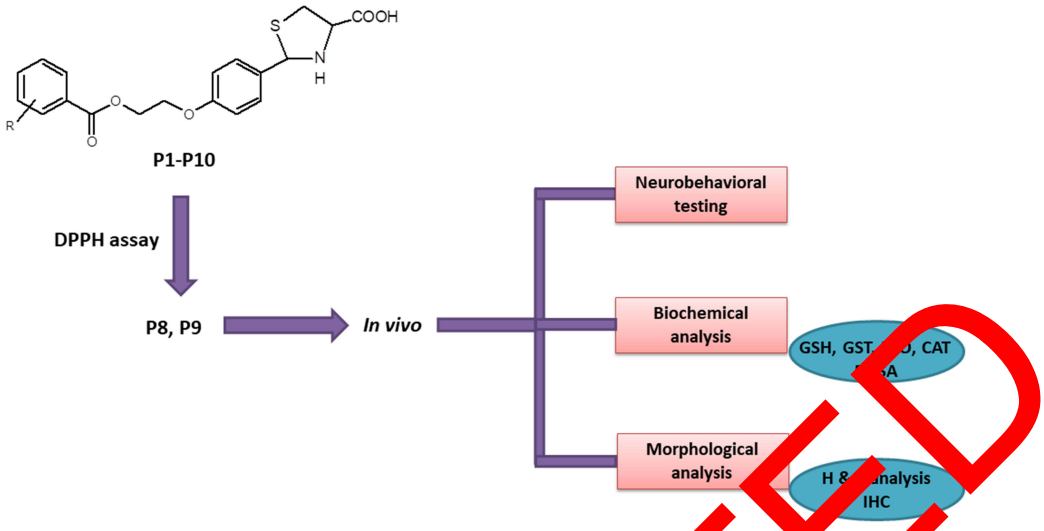

oxidative stress and free radical formation, neuroinflammation, protein misfolding and aggregation, impaired bioenergetics, and mitochondrial dysfunction.[6,7]

Despite the high prevalence, limited or no disease-modifying therapy (DMT) is available for the management of these disorders, and thus emphasizes a marked translational gap from drug development to in vivo experimentation and to clinical trials.[8,9] Several heterocyclic moieties such as thiazolidine show remarkable biological activities due to the innate structural diversity, which offers structure modulation to a greater extent.[10,11] Many thiazolidines are available as potential clinical drugs against many diseases; such as pioglitazone (antidiabetic), rosiglitazone (antidiabetic), etozoline (loop diuretic), ralitoline (anticonvulsant), teneligliptin (antidiabetic) and benzylpenicillin (antibiotic).[12,13] Furthermore, many thiazolidines are screened for their potential anti-inflammatory, antiviral, anticancer, antimicrobial, acetyl/butyrylcholinesterase inhibition, neuroprotective, antinociceptive, immunostimulant, and hepatoprotective properties.[12,14–19] Likely, these compounds exhibited potent-free radical scavenging properties as demonstrated in several reports[20–24] which can be attributed to neuroprotection in Parkinson's[25,26] Alzheimer's,[27] and other memory impairment models.[28] In this context, the beneficial effects of thiazolidines against multiple Alzheimer's targets have been recently reviewed.[28–30] Previously reported mechanistic studies showed that thiazolidines mediate anti-inflammatory effects by inhibition of NF-κB.[31,32]

As cited in most of the scientific literature, the ethanol-induced model of neurodegeneration is widely used since it covers the majority of aspects of both memory impairment and neuroinflammation.[33,34] Neuroinflammation is a common attribute of all neurological disorders, triggered by oxidative stress and excites altered neuronal function.[35,36] The surge in inflammatory mediators and cytokines causes the penetration of macrophages into the brain, which further exacerbates the underlying pathogenesis.[37] Similarly, other research studies also implicated the role of inflammatory cascades in the pathophysiology of various neurodegenerative models not in laboratory animals but also in postmortem brain samples.[38,39] Furthermore, inflammatory cytokines trigger behavioral and cognitive deficits[40] impair neurotransmitter metabolism, and decrease neuroplasticity.[41,42] Furthermore, behavioral and cognitive alteration by ethanol consumption in humans are replicated in animal rodent models. Based on these shreds of evidence, we used ethanol to induce neuroinflammation, neurodegeneration, and behavioral deficits and thereby use it as a model of memory impairment.[35] Furthermore, alcohol consumption can exacerbate the underlying pathology of many neurological disorders such as Alzheimer's disease, depression, and memory loss[43] both by expedites cytokines release and also compromises the endogenous antioxidant defense system[44] and therefore can induce neuronal death either by apoptosis or necrosis (or even both).[45]

The NLRP3 inflammasome plays a significant role in innate immunity and is, therefore, the most investigated inflammasome[46] Mitochondrial dysfunction has been suggested to accelerate neurodegeneration due to elevated reactive oxygen species (ROS) production and NLRP3 inflammasome activation in neurodegenerative and other inflammatory diseases.[47] Activation of NLRP3 inflammasome involves a two-step process. First, the activation of the nuclear factor-kappa B (NF-κB) pathway is required to upregulate the expression of NLRP3, pro-interleukin-1β (pro-IL-1β), and caspase 1, which is accomplished by stimulating toll-like receptors (TLRs).[48,49] After priming, the NLRP3 complex can be activated by several stimuli, including extracellular ATP, ionic flux, lysosomal rupture, and reactive oxygen species (ROS).[50,51]

Keeping in view the antioxidant, anti-inflammatory, and neuroprotective profile of thiazolidine derivatives, here in this research work, we synthesized new analogs of thiazolidine-4-carboxylic acid, performed its structural analysis, and further evaluated its effect on oxidative stress and neuroinflammation. The results will further add to and evidence our approach to the potential of thiazolidine-4-carboxylic acid for the treatment of memory impairment such as Alzheimer's disease.

Materials and Methods

Experimental Animals

Male adult Sprague Dawley rats of 250–275 g weight and 10–13 weeks of age were obtained from the internally established animal house facility of Riphah International University (FPS-RIU). All the animals were provided with standard controlled environmental conditions of dark/light cycle, 22 ± 2 °C temperature, and humidity (45–55%). This in-house facility was further provided with suitable food and water supply according to the standard protocol. The ethical approval was obtained from Research and Ethics Committee (REC), Riphah International University following authorization number REC/RIPS/2018/17 and guidelines of the Institute of Laboratory Animal Resources, Commission on Life Sciences University, National Research Council (1996) were followed.

Chemicals

All the research chemicals were purchased from Daejung (South Korea), Sigma-Aldrich (St. Louis, MO, USA), and Alfa-Aesar (Germany). Digital Gallenkamp (Sanyo) was used to record the melting points of all the final products and were uncorrected. FTIR spectrophotometer (Alpha Bruker, ATR eco ZnSe, ν_{max} in cm^{-1}) was used to evaluate functional groups of synthesized products. ^{1}H NMR and ^{13}C NMR spectra were recorded using *Bruker AM*300 spectrophotometer in DMSO-d_6 at 300 *MHz* and 75 *MHz* respectively using TMS (Tetramethyl silane) as an internal standard. LECO-183 CHN analyzer was used for elemental analysis. The progress of all reactions was monitored using thin-layer chromatography (TLC). Column chromatographic technique was used to purify the final products using silica gel HF-254 (Merck) and chloroform as eluent. All research chemicals used were of high-purity grade (99% HPLC). Rat NLRP3 Elisa kit (ab277086) was procured from Abcam, UK while Elisa COX-2 kit (Cat # 30205Ra) was purchased from Nanjing Pars Biochem CO., LTD. Rat TNF-a (Cat# E-EL-R0019) were purchased from Elabscience.

Synthesis of Thiazolidine-4-Carboxylic Acid Derivatives (P1-P10)

Synthesis of p-(2-Bromoethyloxy)benzaldehyde (A)

p-Hydroxybenzaldehyde (0.0035 mol) and 1,2-dibromoethane (0.035 mol) were dissolved in 70 mL of dimethylformamide (DMF). Potassium carbonate (0.035 mol) was added and the mixture was stirred for 5 days in the dark at room temperature. The completion of the reaction was checked by TLC and solid potassium carbonate (K_2CO_3) was removed by filtration. Then, DMF and excess dibromoethane were evaporated in a vacuum, the resulting residue was dissolved in chloroform and the solid was again removed. After evaporation of chloroform, the crude product (liquid) was purified by silica-gel column chromatography using chloroform as the eluent to give a light yellow pure solid product **A**.[52]

General Procedure for the Synthesis of Ester Derivatives (C1-C10)

0.0L mol of compound **A** was dissolved in 25 mL of DMF. After that substituted benzoic acids **B1-B10** (0.01 mol), triethylamine (0.01 mol), and potassium iodide (0.01 mol) were added and the mixture was stirred overnight at room temperature. Completion of the reaction was checked by TLC and the mixture was poured into finely crushed ice by stirring and extracted with ethyl acetate (4×25 mL). The combined organic layer was washed with 5% K_2CO_3 and finally

with an aqueous NaCl solution. The organic layer was dried over anhydrous magnesium sulfate, filtered and the solvent was removed under reduced pressure to afford the crude products **C1-C10**.[53] Then, the compounds **C1-C10** were purified by silica gel column chromatography (n-hexane: ethyl acetate 3:1).

General Procedure for the Synthesis of Thiazolidine-4-Carboxylic Acid Derivatives (P1-P10)

Compounds **C1-C10** (1.1 equiv) in 95% ethanol (200 mL) were added in one portion to the solution of L-cysteine hydrochloride hydrate and $NaHCO_3$ (1.1 equiv) in water (200 mL). The reaction mixture was stirred for 6 hours at room temperature. The resultant solid was filtered, washed with ethanol, and dried to afford the desired products **P1-P10** (Figure 1).[16] The compounds were further purified by silica gel column chromatography (n-hexane: ethyl acetate 3:1).

Spectral Analysis

(2*RS*, 4*R*)-2-{4-[2-(Benzoyloxy)ethoxy]phenyl}-1,3-Thiazolidine-4-Carboxylic Acid (P1)

Off-white solid; yield: 76%; m.p. 153–156 °C; R_f = 0.67 (n-hexane:ethyl acetate 3:1); FTIR (ν_{max} cm^{-1}) 3148 (O-H, COOH), 2956 (Sp^2 C-H), 1738 (C=O ester), 1644 (C=O, COOH), 1592 (C=C, aromatic), 1316 (C-N); ^{1}H NMR (DMSO-d_6) δ ppm 10.24, 9.88 (s, 1H, COOH), 8.05–6.98 (m, 18H, Ar-H), 5.61, 5.42 (s, 1H, thiazolidine H-2), 4.64–4.60 (m, 8H, OCH_2CH_2O), 4.49 (dd, *J*=4.5*Hz*, 8.7*Hz*, 1H, thiazolidine H-4), 4.35 (dd, *J*=5.1*Hz*, 9.1*Hz*, 1H, thiazolidine H-4), 3.3–3.29 (m, 4H, thiazolidine H-5); ^{13}C NMR (DMSO-d_6) δ ppm 172.7, 172.3, 167.2, 166.8, 156.3, 155.5, 138.2, 131.7, 131.1, 129.5, 129.2, 128.2, 127.7, 125.1, 124.8, 121.5, 120.9, 115.6, 115.2, 70.8, 70.3, 67.2, 65.8, 65.5, 63.5, 63.1, 42.2, 41.5; Anal. calcd for $C_{19}H_{19}NO_5S$ (373.42): C, 61.11; N, 3.75; H, 5.13. Found: C, 60.72; N, 3.76; H, 4.97%

(2*RS*, 4*R*)-2-(4-{2-[(4-Chlorobenzoyl)oxy]ethoxy}phenyl)-1,3-Thiazolidine-4-Carboxylic Acid (P2)

White solid; yield: 83%; m.p. 141–143 °C; R_f = 0.55 (n-hexane:ethyl acetate 3:1); FTIR (ν_{max} cm^{-1}) 3136 (O-H, COOH), 2975 (Sp^2 C-H), 1732 (C=O ester), 1675 (C=O, COOH), 1595 (C=C, aromatic), 1337 (C-N); ^{1}H NMR (DMSO-d_6) δ ppm 9.88 (s, 2H, COOH), 8.05–6.92 (m, 16H, Ar-H), 5.62, 5.54 (s, 2H, thiazolidine H-2), 4.63–4.57 (m, 8H, OCH_2CH_2 O), 4.45 (dd, *J*=4.5*Hz*, 9.0*Hz*, 1H, thiazolidine H-4), 4.3[illegible] *J*=5.1*Hz*, [illegible]*Hz*, 1H, thiazolidine H-4), 3.39, 3.34 (m, 4H,

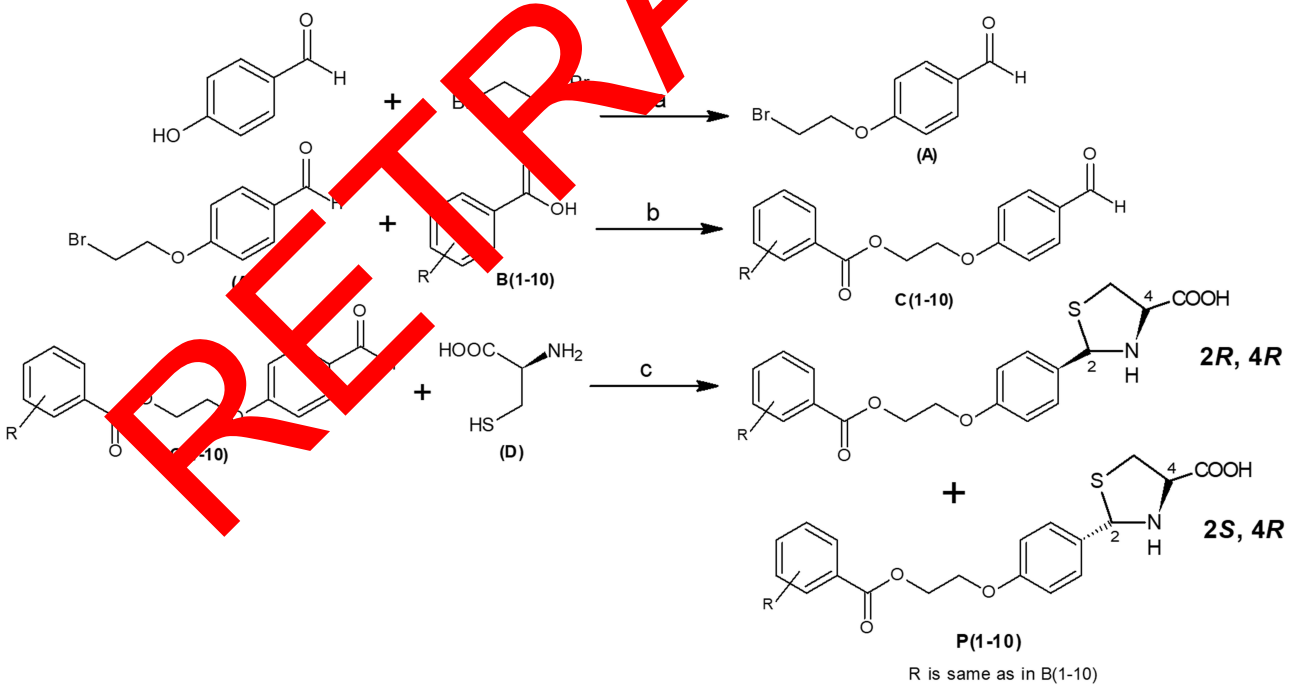

R= B1: H, B2: 4-Cl, B3: 4-F, B4: 4-Br, B5: 4-I, B6: 4-NO2, B7: 4-OCH3, B8: 4-OH, B9: 3-OH, B10: 3-Br

Reagents: (a) K_2CO_3, DMF; (b) $(C_2H_5)_3N$/KI, DMF; (c) $NaHCO_3$, EtOH/H_2O.

Figure 1 Synthesis of thiazolidine-4-carboxylic acid derivatives.

thiazolidine H-5); ^{13}C NMR (DMSO-d_6) δ ppm 173.2, 172.6, 166.4, 165.3, 163.5, 162.6, 158.7, 158.2, 134.7, 133.2, 131.1, 129.4, 128.3, 128.0, 120.6, 120.3, 116.7, 115.8, 114.8, 114.2, 69.5, 69.0, 66.2, 65.7, 64.9, 64.5, 63.6, 63.2, 40.4, 40.1; Anal. calcd for $C_{19}H_{18}ClNO_5S$ (407.87): C, 55.95; N, 3.43; H, 4.45. Found: C, 55.10; N, 3.16; H, 4.32%.

(2*RS*, 4*R*)-2-(4-{2-[(4-Fluorobenzoyl)oxy]ethoxy}phenyl)-1,3-Thiazolidine-4-Carboxylic Acid (P3)

Off-white solid; yield: 88%; m.p. 164–167 °C; R_f = 0.58 (n-hexane:ethyl acetate 3:1); FTIR (ν_{max} cm^{-1}) 3159 (O-H, COOH), 2963 (Sp^2 C-H), 1736 (C=O ester), 1637 (C=O, COOH), 1593 (C=C, aromatic), 1312 (C-N); ^{1}H NMR (DMSO-d_6) δ ppm 9.88 (s, 2H, COOH), 8.03–6.96 (m, 16H, Ar-H), 5.60, 5.45 (s, 1H, thiazolidine H-2), 4.65–4.59 (m, 8H, O*CH*$_2$*CH*$_2$O), 4.49 (dd, *J*=4.5*Hz*, 9.0*Hz*, 1H, thiazolidine H-4), 4.36 (dd, *J*=5.1*Hz*, 9.3*Hz*, 1H, thiazolidine H-4), 3.36, 3.35 (m, 4H, thiazolidine H-5); ^{13}C NMR (DMSO-d_6) δ ppm 173.5, 172.6, 166.1, 165.9, 163.6, 162.7, 157.9, 157.2, 133.7, 133.1, 131.0, 130.8, 129.1, 128.7, 120.9, 120.3, 116.5, 116.0, 115.0, 114.6, 71.6, 71.2, 66.8, 65.7, 64.0, 63.8, 63.5, 63.0, 40.8, 40.4; Anal. calcd for $C_{19}H_{18}FNO_5S$ (391.41): C, 58.30; N, 3.58; H, 4.64. Found: C, 57.95; N, 3.44; H, 4.25%.

(2*RS*, 4*R*)-2-(4-{2-[(4-Bromobenzoyl)oxy]ethoxy}phenyl)-1,3-Thiazolidine-4-Carboxylic Acid (P4)

Off-white solid; yield: 78%; m.p. 159–161 °C; R_f = 0.63 (n-hexane:ethyl acetate 3:1); FTIR (ν_{max} cm^{-1}) 3125 (O-H, COOH), 2956 (Sp^2 C-H), 1733 (C=O ester), 1645 (C=O, COOH), 1595 (C=C, aromatic), 1312 (C-N); ^{1}H NMR (DMSO-d_6) δ ppm 10.31, 9.87 (s,1H, COOH), 8.24, 6.83 (m, 16H, Ar-H), 5.61, 5.54 (s, 1H, thiazolidine H-2), 4.61–4.60 (m, 8H, O*CH*$_2$*CH*$_2$O), 4.48 (dd, *J*=4.2*Hz*, 9.0*Hz*, 1H, thiazolidine H-4), 4.32 (dd, *J*=5.3*Hz*, 9.1*Hz*, 1H, thiazolidine H-4), 3.38–3.29 (m, 4H, thiazolidine H-5); ^{13}C NMR (DMSO-d_6) δ ppm 173.5, 172.1, 165.8, 163.2, 162.7, 157.7, 157.3, 135.3, 134.8, 132.1, 131.6, 129.3, 128.7, 121.5, 120.9, 117.4, 117.0, 114.7, 114.3, 69.9, 69.2, 66.5, 66.4, 65.8, 65.1, 63.4, 62.9, 40.6, 40.2; Anal. calcd for $C_{19}H_{18}BrNO_5S$ (452.32): C, 50.45; N, 3.10; H, 4.01. Found: C, 50.37; N, 3.04; H, 3.89%.

(2*RS*, 4*R*)-2-(4-{2-[(4-Iodobenzoyl)oxy]ethoxy}phenyl)-1,3-Thiazolidine-4-Carboxylic Acid (P5)

Yellow Off-white solid; yield: 73%; m.p. 185–188 °C; R_f = 0.61 (n-hexane:ethyl acetate 3:1); FTIR (ν_{max} cm^{-1}) 3142 (O-H, COOH), 2951 (Sp^2 C-H), 1725 (C=O ester), 1630 (C=O, COOH), 1582 (C=C, aromatic), 1323 (C-N); ^{1}H NMR (DMSO-d_6) δ ppm 10.28, 9.88 (s,1H, COOH), 7.99–6.82 (m, 16H, Ar-H), 5.60, 5.46 (s, 1H, thiazolidine H-2), 4.62–4.60 (m, 8H, O*CH*$_2$*CH*$_2$O), 4.45 (dd, *J*=4.5*Hz*, 9.1*Hz*, 1H, thiazolidine H-4), 4.36 (dd, *J*=5.6*Hz*, 9.3*Hz*, 1H, thiazolidine H-4), 3.36–3.27 (m, 4H, thiazolidine H-5); ^{13}C NMR (DMSO-d_6) δ ppm 173.3, 172.8, 167.2, 166.6, 163.5, 163.0, 156.1, 155.7, 134.3, 134.1, 131.9, 131.3, 129.6, 128.3, 120.2, 117.5, 116.8, 114.6, 114.2, 70.2, 69.7, 67.4, 67.1, 65.7, 65.0, 63.8, 63.3, 40.9, 40.1; Anal. calcd for $C_{19}H_{18}INO_5S$ (499.31): C, 45.70; N, 2.81; H, 3.63. Found: C, 45.26; N, 2.57; H, 3.39%.

(2*RS*, 4*R*)-2-(4-{2-[(4-Nitrobenzoyl)oxy]ethoxy}phenyl)-1,3-Thiazolidine-4-Carboxylic Acid (P6)

Light yellow solid; yield: 82%; m.p. 184–186 °C; R_f = 0.48 (n-hexane:ethyl acetate 3:1); FTIR (ν_{max} cm^{-1}) 3148 (O-H, COOH), 2963 (Sp^2 C-H), 1729 (C=O ester), 1674 (C=O, COOH), 1590 (C=C, aromatic), 1315 (C-N); ^{1}H NMR (DMSO-d_6) δ ppm 9.88 (s, 2H, COOH), 8.36–6.82 (m, 16H, Ar-H), 5.64, 5.46 (s, 1H, thiazolidine H-2), 4.62–4.61 (m, 8H, O*CH*$_2$*CH*$_2$O), 4.49 (dd, *J*=4.2*Hz*, 9.0*Hz*, 1H, thiazolidine H-4), 4.35 (dd, *J*=5.6*Hz*, 9.3*Hz*, 1H, thiazolidine H-4), 3.38–3.27 (m, 4H, thiazolidine H-5); ^{13}C NMR (DMSO-d_6) δ ppm 173.4, 172.8, 166.8, 166.0, 164.6, 163.7, 150.7, 150.2, 135.2, 134.8, 132.3, 131.9, 131.9, 130.3, 129.5, 124.4, 124.2, 115.5, 114.8, 71.5, 71.0, 66.6, 66.3, 64.4, 63.9, 63.2, 62.8, 40.8, 40.2; Anal. calcd for $C_{19}H_{18}N_2O_7S$ (418.42): C, 54.54; N, 6.70; H, 4.34. Found: C, 54.12; N, 6.38; H, 4.26%.

(2*RS*, 4*R*)-2-(4-{2-[(4-Methoxybenzoyl)oxy]ethoxy}phenyl)-1,3-Thiazolidine-4-Carboxylic Acid (P7)

White solid; yield: 77%; m.p. 149–151 °C; R_f = 0.52 (n-hexane:ethyl acetate 3:1); FTIR (ν_{max} cm^{-1}) 3145 (O-H, COOH), 2969 (Sp^2 C-H), 1732 (C=O ester), 1644 (C=O, COOH), 1597 (C=C, aromatic), 1331 (C-N); ^{1}H NMR (DMSO-d_6) δ ppm 9.92, 9.84 (s, 1H, COOH), 7.98–6.82 (m, 16H, Ar-H), 5.61, 5.50 (s, 1H, thiazolidine H-2), 4.62–4.60 (m, 8H, O*CH*$_2$ *CH*$_2$O), 4.47 (dd, *J*=4.5*Hz*, 9.0*Hz*, 1H, thiazolidine H-4), 4.34 (dd, *J*=5.1*Hz*, 9.1*Hz*, 1H, thiazolidine H-4), 3.38–3.35 (m, 4H, thiazolidine H-5), 3.27, 3.22 (s, 3H, OCH_3); ^{13}C NMR (DMSO-d_6) δ ppm 173.8, 173.2, 167.5, 166.9, 163.7, 162.5, 158.4, 158.1, 135.7, 135.2, 132.2, 131.8, 129.3, 128.9, 120.5, 120.1, 117.5, 117.2, 115.6, 114.9, 69.2, 68.5, 66.6, 66.3, 64.3, 64.1, 63.9, 63.0, 41.4, 41.2; Anal. calcd for $C_{20}H_{21}NO_6S$ (403.44): C, 59.54; N, 3.47; H, 5.25. Found: C, 58.63; N, 3.35; H, 5.10%.

(2*RS*, 4*R*)-2-(4-{2-[(4-Hydroxybenzoyl)oxy]ethoxy}phenyl)-1,3-Thiazolidine-4-Carboxylic Acid (P8)

White solid; yield: 80%; m.p. 167–170 °C; R_f = 0.41 (n-hexane:ethyl acetate 3:1); FTIR (ν_{max} cm^{-1}) 3265 (O-H, aryl), 3125 (O-H, COOH), 2972 (Sp^2 C-H), 1735 (C=O ester), 1656 (C=O, COOH), 1586 (C=C, aromatic), 1339 (C-N); ^{1}H NMR (DMSO-d_6) δ ppm 10.31, 9.88 (s,1H, COOH), 7.89–6.83 (m, 16H, Ar-H), 5.60, 5.45 (s, 1H, thiazolidine H-2), 4.58–4.52 (m, 8H, OCH_2CH_2O), 4.45 (dd, *J*=4.5*Hz*, 8.7*Hz*, 1H, thiazolidine H-4), 4.33 (dd, *J*=5.1*Hz*, 9.3*Hz*, 1H, thiazolidine H-4), 3.39–3.28 (m, 4H, thiazolidine H-5); ^{13}C NMR (DMSO-d_6) δ ppm 173.5, 172.7, 165.9, 165.9, 163.7, 162.5, 158.7, 158.2, 133.6, 132.3, 132.0, 131.5, 129.1, 128.8, 120.5, 120.4, 115.8, 115.5, 115.0, 114.7, 71.9, 71.3, 66.9, 66.4, 65.8, 65.2, 63.2, 63.0, 40.7, 40.5; Anal. calcd for $C_{19}H_{19}NO_6S$ (389.42): C, 58.60; N, 3.60; H, 4.92. Found: C, 58.12; N, 3.54; H, 4.85%.

(2*RS*, 4*R*)-2-(4-{2-[(3-Hydroxybenzoyl)oxy]ethoxy}phenyl)-1,3-Thiazolidine-4-Carboxylic Acid (P9)

White solid; yield: 83%; m.p. 162–165 °C; R_f = 0.40 (n-hexane:ethyl acetate 3:1); FTIR (ν_{max} cm^{-1}) 32[illegible] (O-H, aryl), 3136 (O-H, COOH), 2985 (Sp^2 C-H), 1733 (C=O ester), 1637 (C=O, COOH), 1593 (C=C, aromatic), 1[illegible]23 (C-N); ^{1}H NMR (DMSO-d_6) δ ppm 9.88, 9.84 (s,1H, COOH), 7.89–6.84 (m, 16H, Ar-H), 5.62, 5.45 (s, [illegible]H, thiazolidine H-2), 4.62–4.55 (m, 8H, OCH_2CH_2O), 4.45 (dd, *J*=4.5*Hz*, 9.0*Hz*, 1H, thiazolidine H-4), [illegible].35 (dd, *J*=[illegible]3*Hz*, 9.1*Hz*, 1H, thiazolidine H-4), 3.39–3.35 (m, 4H, thiazolidine H-5); ^{13}C NMR (DMSO-d_6) δ ppm 17[illegible].8, 173.[illegible], 167.5, 167.1, 163.5, 162.7, 156.2, 155.8, 134.8, 134.3, 131.4, 131.0, 129.3, 128.8, 121.8, 1[illegible].4, [illegible].6, 116.0, [illegible]14.5, 114.2, 70.6, 69.8, 67.4, 66.9, 65.7, 65.3, 63.5, 63.0, 40.2, 39.9; Anal. calcd for $C_{19}H_{19}N$[illegible]S (389.42): C, 5[illegible]60; N, 3.60; H, 4.92. Found: C, 58.21; N, 3.35; H, 4.47%.

(2*RS*, 4*R*)-2-(4-{2-[(3-Bromobenzoyl)oxy]ethoxy}phenyl)-1,3-T[illegible]idine-4-Ca[illegible]oxylic Acid (P10)

Off-white solid; yield: 76%; m.p. 153–157 °C; R_f = 0.62 (n-hex[illegible]ne:ethyl acetate 3:1); FTIR (ν_{max} cm^{-1}) 3139 (O-H, COOH), 2977 (Sp^2 C-H), 1737 (C=O ester), 1642 (C=O, CO[illegible]H), 1590 ([illegible]=C, aromatic), 1312 (C-N); ^{1}H NMR (DMSO-d_6) δ ppm 10.34, 9.88 (s,1H, COOH), 7.98–6.84 (m, 16H, Ar-H), 5.[illegible]1, 5.50 (s, 1H, thiazolidine H-2), 4.58–4.53 (m, 8H, OCH_2CH_2O), 4.48 (dd, *J*=4.5*Hz*, 8.7*Hz*, 1[illegible]t[illegible]olidine H-4), 4.33 (dd, *J*=5.1*Hz*, 9.3*Hz*, 1H, thiazolidine H-4), 3.39–3.32 (m, 4H, thiazolidine H-5); ^{13}C NMR (DM[illegible]O-d_6) [illegible] 174.3, 173.6, 164.7, 164.1, 163.5, 162.3, 158.6, 158.2, 134.2, 133.8, 131.5, 131.0, 129.3, 128.7, [illegible]1.5, 12[illegible], 117.6, 117.3, 115.3, 114.8, 70.5, 70.2, 67.2, 66.8, 65.4, 65.1, 63.9, 63.0, 41.8, 41.1; Anal. calcd for [illegible]$_{19}H_{18}$[illegible]NO_5S [illegible]452.31): C, 50.45; N, 3.10; H, 4.01. Found: C, 49.87; N, 3.06; H, 3.79%.

In vitro Antioxidant Ass[illegible]

The antioxidant activity of the final pro[illegible]cts (P1-P10) was determined by a 2.2-diphenyl-1-picrylhydrazyl (DPPH) free radical scavenging assay.[54] [illegible] solution was [illegible]rmulated containing 3mL DPPH in methanol (1 mL) as a negative control. Similarly, a solution of [illegible]scorbic [illegible]cid was formulated (reference standard). A reaction mixture was prepared by adding 3mL of test compound[illegible] (diff[illegible]ent concentrations) and 1mM DPPH solution (methanol) kept in dark for 30 min and absorbance was [illegible]ated ([illegible]7 nm) [illegible]sing a UV spectrophotometer. All the determinations were carried out in triplicates and average [illegible]lues w[illegible]e consi[illegible]d. The results indicated the antioxidant potential of test compounds. The shift in color from blue t[illegible]yellow[illegible]ge also confirms the antioxidant potential of compounds under observation.

Similarly, t[illegible] change in color (bluish-grey to yellowish-orange) also depicts an experimental indication. Percent radical scavenging [illegible]fficacy was determined using the formula:

$$\%\ \text{radical scavenging} = \left(\frac{\text{the absorbance of control} - \text{absorbance of the test sample}}{\text{absorbance of control}}\right) \times 100$$

In vivo Study Design and Treatments

Based on the results of preliminary in vitro experimentation, two compounds (P8 and P9) were selected among thiazolidine-4-carboxylic acid derivatives (P1-P10) for further in vivo evaluation of pharmacological activities and molecular investigation. Rats with approximately similar weights were assorted in one group under identical test conditions. Five groups comprising 16 rats each were organized into various groups. Group 1 (Control):

Intraperitoneal injection of normal saline, 1 mL/Kg, once a day (11 days), Group 2 (Disease): Intraperitoneal injection of ethanol, 2g/Kg, once a day (11 days), Group 3 (Treatment group P8): Administration of test compound P8 (5 mg/Kg), 30 mins following intraperitoneal injection of ethanol (2g/Kg) once daily (11 days). Group 4 (Treatment group P9): Administration of test compound P9 (5 mg/Kg), 30 mins following intraperitoneal injection of ethanol once daily (11 days), Group 5 (Reference group): Administration of donepezil 3 mg/kg (standard drug), 30 mins following intraperitoneal injection of ethanol once daily (11 days).

Ethanol can be utilized as a neurotoxic agent to induce neurodegeneration in rats.[33] From day 12 onwards, animals in all groups were subjected to behavioral studies and sacrificed according to the standard protocol. The collected cortex and hippocampus were subjected to centrifugation using phosphate buffer saline (pH 7.4). The supernatant was then stored at −80°C for further biochemical analysis. For immunohistochemical staining, brain tissue was stored in formaldehyde (4%), and accordingly for immunohistochemical analysis paraffin blocks were prepared.

Behavioral Tests

Y-Maze Test

A modified Y-shaped tool was employed for the behavioral study of rats in the maze test. The dimensions of the apparatus arms were 20 cm in height, 10 cm wide, and 50 cm in length. The trial was executed in three sessions of 8 min each. Rats were placed at the center of Y-shaped maze and were allowed to move impulsively. Spontaneous alternation behavior was assessed by studying the continuous uninterrupted entry of rats into the arms. The following equation was used to study the percent alteration behavior of rats. Three sessions of this test were performed and the duration of each trial lasted 8 minutes. In this Y-shaped apparatus, each rodent was concisely placed at the central position of this Y-shaped maze and permitted to move spontaneously. All uninterrupted rat entrances to the arms were examined visually. A spontaneous alternation behavior was defined as continuous uninterrupted entry of the rodents into the arms.

$$\text{The alteration behavior } (\%) = \begin{bmatrix} \text{three successive ses} \\ \text{(successive entry of ts in} \quad \text{ee different arms)} \\ \text{/total arm entries} - 2 \end{bmatrix} \times 100.[55]$$

Morris Water Maze (MWM) Test

To evaluate memory function, the MWM test was performed. Previously reported was used to perform this test with minor adjustments.[55] The apparatus was made up of a circular tank (100 cm in diameter, 40 cm in height) containing water to a depth of 15.5 cm at a temperature of 25 ± 1 °C. By adding some white ink, the water was made opaque. At the center of one quadrant, a probe with specifications (10 cm diameter and 20 cm height) was positioned nearly 1 cm below the water surface. For each group, this test was performed for 5 continuous days. Escape latency was determined for all animal groups for 5 days with 4 sessions each day. Usually, the session involved a distinct release position and a platform hidden in a single quadrant. On finding a hidden probe rodent was allowed to stay on it for 10 sec. Rats that cannot locate the probe in 90 sec were also allowed to stay on it for 10 sec.

The escape latency time was estimated for individual sessions. Spatial memory measurements were determined on the 5th day and the session did not involve the use hidden probe during this session. Rats were allowed to swim spontaneously for 60 seconds in a water container to determine the time spent by rats in the target quadrant. Finally, the escape latency time was estimated using video recordings. A decrease in escape latency time corresponded to the attenuation of memory deficits.

Determination of Oxidative Stress Markers

Glutathione (GSH) and Glutathione s-Transferase (GST) Assay

Phenylmethylsulfonyl fluoride (PMSF) was applied to freshly cut and homogenized (0.1M PBS at pH 7.4) brain tissue samples and centrifuged (4000 × g) at 4 °C for 10 minutes. The supernatant layer was separated in a beaker to evaluate the GSH levels using the previously described method with slight modifications.[34] Sodium phosphate solution (0.2M) was used to dissolve DTNB (0.6 mM). The resultant mixture (2mL) was added to 0.2 mL of supernatant. Finally, the

mixture volume was made up to 3 mL using 0.2 M PBS, and the sample mixture was subjected to measure absorbance at 412 nm. PBS and DTNB solutions were used as a negative and positive control, respectively. Results were obtained as µmoles/mg of proteins. Similarly, the Glutathione s-transferase (GST) levels were determined using the previously reported method with some modifications.[36] The test solution was prepared in 0.1 M PBS with GSH (5 mM) and CDNB (1 mM). 60 µL of previously collected supernatant was added into a glass vial containing test solution (1.2 mL). Blanks were prepared in triplicate using water in the same proportion. The sample test solutions were analyzed using the ELISA microplate reader at a wavelength of 340 nm. Results were presented in µmoles/mg of proteins.

LPO Assay

Lipid peroxide assay was used to quantify thiobarbituric acid reactive substances.[56] Supernatant solution (200 µL), 100 mL of ascorbic acid (200 µL) and PBS (580 µL, pH 7.4, 0.1 M), and ferric chloride (20 µL) were mixed and incubated for 1 hr in a water bath at 37°C. This was followed by the addition of 0.66% of thiobarbituric acid (1000 µL) and 10% trichloroacetic acid (1000 µL) to stop the proceeding reaction. The resultant mixture was again incubated for 20 mins, cooled, followed by centrifugation (3000 × g) for 10 min. The absorbance of measured at 535 nm to estimate the concentration of thiobarbituric acid reactive substances expressed in nM/min/mg of protein.

Catalase Assay

Catalase (CAT) is a common heme-containing enzyme that catalyzes the decomposition of H_2O_2 to H_2O. Catalase activity was measured by monitoring the decrease in absorbance due to decomposition of H_2O_2 at 240 nm according to the previously reported method with minor modifications.[57] A reaction mixture consisting of 1.95 mL of PBS (pH 7.0), 1mL of hydrogen peroxide (H_2O_2), and 0.05mL of supernatant was prepared, and the absorbance was measured at 240 nm. The results were expressed as µmoles of H_2O_2/min/mg of protein.

Immunohistochemical Staining

For immunohistochemical evaluation, a rotary microtome was used to slice coronal tissue according to the previously published method.[58] Already prepared tissue slides were treated with xylene solution thrice (5–10 mins) and were rehydrated afterward, using alcohol in a graded sequence (100%; 90%; 80%; 70%). Distilled water was used to wash the slides to get rid of any alcohol. Next, treated with proteinase K followed by subsequent washing with PBS (0.1 M). Slides were treated with H_2O_2-methanol solution (3 mL) for 10 mins and washed again using 0.1 M PBS. Sides were subjected to incubation for 1 hr with 5% natural goat serum, followed by overnight incubation with anti-p-NF-κB and anti-TNF-α (primary rat antibodies) (Santa Cruz Biotechnology, USA) at 4°C. Slides were further incubated with biotinylated secondary antibodies (1:50 for 90 mins) and with subsequent washing with PBS, slides were again incubated in a humidified chamber for another hour with ABC Elite Kit (Santa Cruz Biotechnology, USA). Slides were then stained with 3.3-diaminobenzidine peroxidase (DAB solution), washed with distilled water, dehydrated with various alcohol grades, fixed in xylene, and slips were placed and images were captured using a light microscope (Olympus, Japan).

Enzyme Linked Immunosorbent Assay (ELISA)

The expressions of NLRP3, TNF-α, and COX-2 were measured using rat ELISA kits as per the manufacturer's instructions. Brain tissue (50 mg) was homogenized (1500 rpm) in PBS (2500 µL) containing phenylmethylsulfonyl fluoride-PMSF (a protease inhibitor). The mixture was subjected to centrifugation (10 min at 4000 × g) and the supernatant was collected. Total protein content was estimated using the BCA method and protein expression was determined by the addition of equivalent protein quantities. Expressions of NLRP3, TNF-α, and COX-2 were investigated using an ELISA microplate reader (BioTekELx808) and total protein content was expressed as pg/mg of total protein.

Molecular Docking

Molecular docking analysis predicts the binding affinity, binding pose, and interactions of ligands in the binding pocket of the target proteins using Autodock Vina (4.2.6) software (San Diego, CA, USA). 3D crystallographic structures of

selected proteins NF-κB (PDB ID: 1VSC), TLR4 (2Z65), NLRP3 (6NPY) and COX-2 (3LN1) were downloaded from RCSB Protein Data Bank http://www.rscb.org/pdb. DoGSiteScorer was used to predict the active sites of proteins.[59] Protein structures were prepared for docking using Accelrys Discovery Studio Visualizer (version 4.1) and saved as PDBQT files by AutoDock Tools (version 1.5.6). Water molecules and co-crystallized ligands were removed from the ligand-protein complex and saved as PDB files. The structures of synthesized compounds and reference ligands were sketched using the ChemSketch tool and saved as Mol. files. 3D structures of the ligands were generated by Open Babel software.[60] Furthermore, PDB structures of compounds and reference ligands after adding torsions and saved as PDBQT files. Finally, docking calculations of ligands-protein complexes were done by AutoDock Vina 4.2.6, a virtual screening software to calculate energies.[61] In addition, the ligand–protein interactions were visualized using Accelrys Discovery Studio Visualizer (version 4.1).

Statistical Analysis

All the data presented has been evaluated using one-way analysis of variance (ANOVA) and expressed as mean ±SEM (standard error of the mean). Graph pad prism (version 6.0) was used for posthoc Bonferroni multiple comparisons. Two-way analysis of variance was utilized for grouped analysis for behavioral analysis and data with a p value less than 0.05 was considered to be statistically significant. "#" represented a significant difference vs the saline group, whereas the symbol "*" indicated a significant difference vs the disease group.

Results

Chemistry

Ten new derivatives of thiazolidine-4-carboxylic acid were synthesized using the scheme given in Figure 1. In the first step, 4-hydroxybenzaldehyde was converted to ether derivative p-(2-Bromoethyloxy)benzaldehyde **(A)** upon reaction with 1.2-dibromoethane. Secondly, compound A was reacted with different substituted carboxylic acids **(B1-B10)** to afford respective esters **(C1-C10)**. Ester bond formation was confirmed by the appearance of carbonyl stretch ranging from 1738 cm^{-1} - 1725 cm^{-1} in the FTIR spectra. Finally, synthesized esters were condensed with L-cysteine hydrochloride hydrate to yield the respective thiazolidine-4-carboxylic acid final products **(P1-P10)**. This condensation reaction resulted in generation of a new uncontrolled chiral center and the compounds **(P1-P10)** are obtained as inseparable diastereomeric mixtures (2R, 4R: 2S, 4R). Although the 2R, 4R and 2S, 4R isomers were mixed, the appearance of a distinctive singlet around 5.[illegible] ppm in the ^{1}H-NMR spectra for C-2 proton gave a clearly distinguishable ratio of the isomers. While the signal for C-2 carbon atom around 70.5 ppm in ^{13}C-NMR spectra further confirmed the results.

In vitro Antioxidant Assay

The antioxidant results for compounds (P1-P10) are shown in Figure 2. All the newly synthesized compounds showed antioxidant potential to variable extent but two compounds P8 and P9 showed significant activities with an EC_{50} value of 12.16 µg/mL and 13.9 µg/mL, respectively, relative to ascorbic acid (10.14 µg/mL). This effect might be due to the availability of phenolic fragments in the structures of selected compounds **P8** and **P9**. The hydroxyl group additionally contributes to the inhibition of the DPPH radical, and the resulting cation radical is stabilized by the delocalization of the electron across the molecule.

Molecular Docking Results

Newly synthesized thiazolidine-4-carboxylic acid derivatives **(P1-P10)** and co-crystallized ligands were docked into active sites of NF-κB, NLRP3, TLR4, and COX-2 that have a significant role in neuroinflammation. The binding energies of docked ligands are presented in Table 1. Docking scores demonstrated that compounds **P8** and **P9** showed a comparatively greater binding affinity with all the targets. Docking results of compounds **P8** and **P9** with COX-2 are presented in Figure 3A and B. Compound **P9** (Figure 3B) showed a greater binding affinity (−8.9 kcal/mol) than P8 (Figure 3A; −8.5 kcal/mol) relative to the standard celecoxib (−8.0 kcal/mol). Compound P8 (Figure 3A, **Panel b)** was stabilized into the active site of COX-2 through five hydrogen bonds. Three hydrogen bonds were formed by the

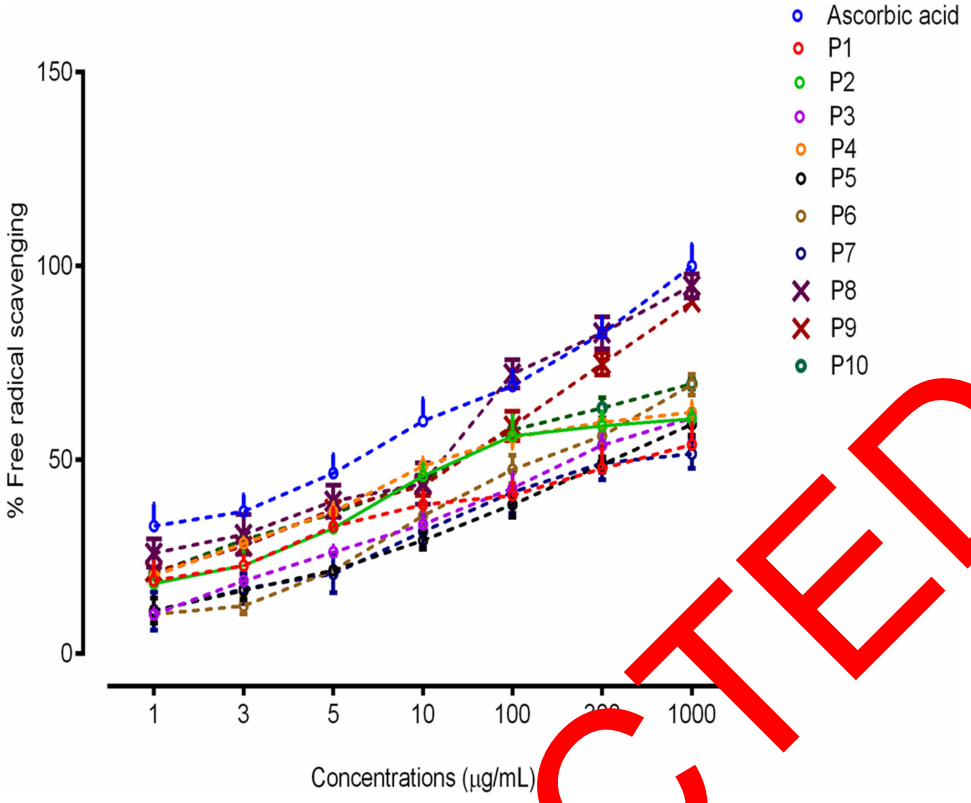

Figure 2 Antioxidant potential of all synthesized compounds (P1-P10) using DPPH assay. The presence of phenolic groups in compounds P8 and P9 contributed to the inhibition of DPPH radicals.

carboxylic acid group, one by the N-H group of thiazolidine as hydrogen bond donor (HBD) and one by the carbonyl group of ester moiety as hydrogen bond acceptor (HBA). Pi-sigma interactions were observed between the phenyl ring and LeuC:131. Moreover, the complex was stabilized by several Van Der Waals interactions. The interaction of

Table 1 Binding Energy Values after Docking. COX, Cyclooxygenase; p-NF-κB, Nuclear Factor-κB; TLR4, Toll-Like Receptors; NLRP3, Pyrin Domain-Containing Protein 3

Compound	COX-1	NF-κB	TLR4	NLRP3
	Binding Energies (Kcal/mol)			
P1	−8.1	−6.1	−6.5	−7.6
P2	−8.0	−5.2	−6.4	−7.6
P3	−7.8	−5.7	−6.2	−7.1
P4	−6.5	−5.4	−5.9	−7.0
P5	−7.6	−5.2	−6.0	−7.1
P6	−8.3	−5.5	−6.2	−7.3
P7	−7.0	−6.0	−6.1	−7.5
P8	−8.4	−6.1	−6.6	−8.0
P9	−8.9	−6.4	−6.8	−8.2
P10	−7.8	−6.0	−6.3	−7.9
CO-crystal	−8.5		−7.1	

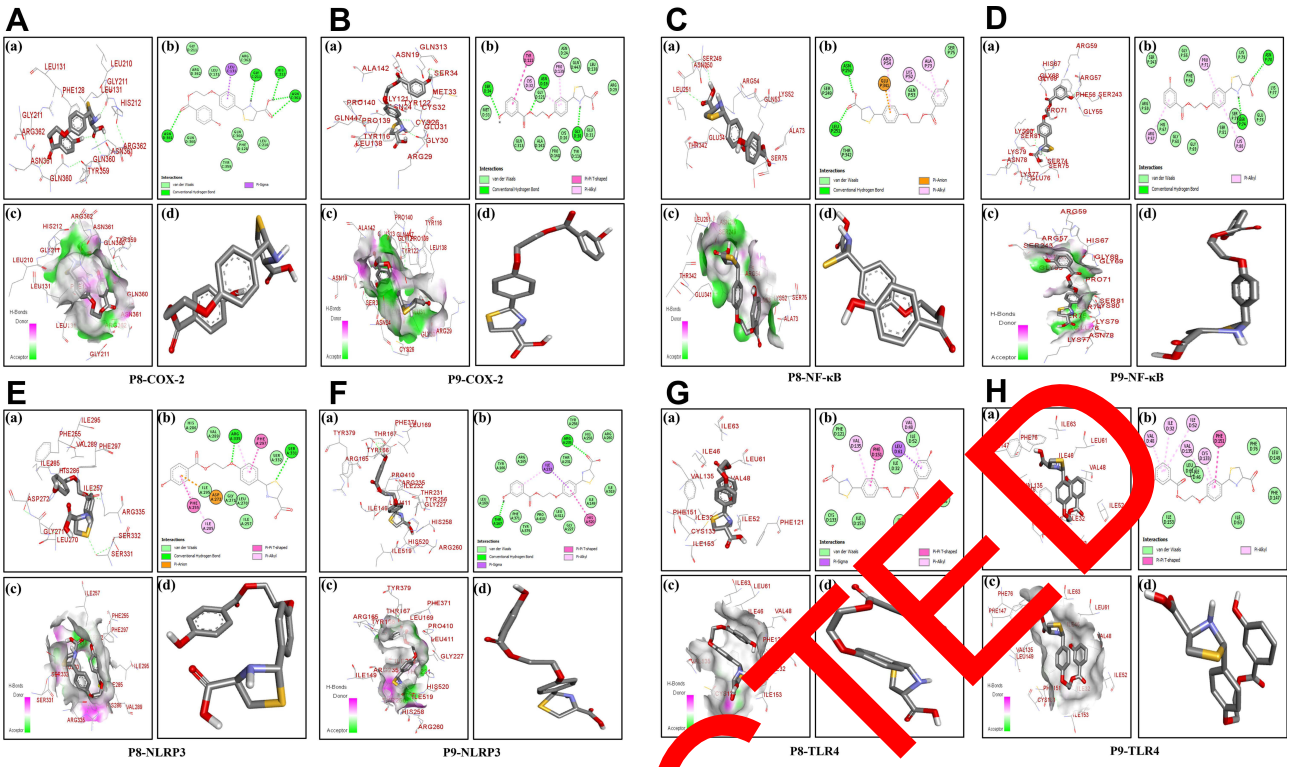

Figure 3 Post docking analysis visualized by Discovery Studio Visualizer in both 2D and 3D poses in the protein structures of COX-2. Interaction between P8 and COX-2 (**A**), P9 and COX-2 (**B**). Post docking analysis visualized by Discovery Studio Visualizer in both 2D and 3D poses in the protein structures of NF-κB. Interaction between P8 and NF-κB (**C**), P9 and NF-κB (**D**). Post docking analysis visualized by Discovery Studio Visualizer in both 2D and 3D poses in the protein structures of NLRP3. Interaction between P8 and NLRP3 (**E**), P9 and NLRP3 (**F**). Post docking analysis visualized by Discovery Studio Visualizer in both 2D and 3D poses in the protein structures of TLR4. Interaction between P8 and TLR4 (**G**), P9 and TLR4 (**H**). In all these figures (panel a) represents 3D pose, (panel b) represents 2D interactions, (panel c) represents 2D hydrogen bonds, and (panel d) represents 2D-PDB binding mode.

compound **P9** with COX2 (Figure 3B, **panel b**) showed three hydrogen bonds, one by the oxygen of ester moiety as HBA, second by the N-H group of thiazolidine nucleus while the third hydrogen bond was observed by the para hydroxyl group as HBA Furthermore, pi-alkyl interactions were shown by phenyl ring attached to thiazolidine nucleus with Cyc32 and Pro139 of chain D. The phenyl ring attached to ester moiety formed pi–pi interaction with TyrD:122. The complex was further stabilized by Van Der Waals's interactions.

Figure 3C and D shows the docking results of compounds **P8** and **P9** with NF-κB. Compounds **P8** and **P9** bind to the active site of NF-κB with binding energy values of −5.3 kcal/mol and −6.4 kcal/mol respectively. The carboxylic acid group of compound P8 (Figure 3C, **Panel b**) formed two hydrogen bonds with the target protein. Moreover, both phenyl rings were involved in pi-anion and pi–alkyl interactions with Leu341, Lys52, Arg54, and Ala73, respectively. Further stabilization was provided by Van Der Waals's interactions. Compound **P9** (Figure 3D, **Panel b**) was stabilized by hydrogen bonds, pi-alkyl and Van Der Waals interactions. The carbonyl group of ligand formed one hydrogen bond with Asn78 as HBA while the N-H group of thiazolidine scaffold showed one hydrogen bond with Ser74. The interactions of compounds **P8** and **P9** with NLRP3 are presented in Figure 3E and F. The binding energies of compounds **P8** and **P9** with NLRP3 were −7.9 kcal/mol and −8.0 kcal/mol, respectively. One hydrogen bond was observed between sulphur of compound **P8** and Ser331 as HBA and another hydrogen bond between the oxygen of ether with Arg335 as HBA (Figure 3E, **panel b**). In contrast, compound **P9** (Figure 3F, **Panel b**) formed two hydrogen bonds, one between the carbonyl group of carboxylic acid moiety and Arg235, and another hydrogen bond was formed by the para hydroxyl group with Thr167. Figure 3G and H shows the docking results of test compounds with TLR4. Compound **P8** was stabilized by pi–alkyl interactions with Val48, Val135, pi–sigma interactions with Leu61, pi–pi interactions with Phe151, and Van Der Waals interactions (Figure 3G, **Panel b**). Compound **P9** showed pi–alkyl interactions with Ile32, Val48,

Ile52, Cys133, and Val135. Moreover, pi–pi interactions with Phe151 and Van Der Waals interactions further stabilized the complex (Figure 3H, **Panel b**).

Effect of Thiazolidine Derivatives (P8 & P9) on Cognitive Impairment and Histopathology

To determine the relative role of our test compounds on cognitive deficits, we performed MWM and Y-maze tests as these tests assess hippocampus-dependent spatial learning. In the hidden-platform test of MWM, ethanol-treated rats exhibited a higher latency time compared with saline-treated rats, which indicated severe memory deficits (Figure 4A, $p < 0.01$). Treatment with **P8** and **P9** at 5 mg/kg doses significantly improved memory deficits and improved the latency time to reach the hidden platform (Figure 4A, $p < 0.05$). Next, we also evaluated the number of crossings and the time spent in the target quadrant, which showed that the number of platform crossings and the time spent in the target quadrant were significantly enhanced in the drug co-treated groups (Figure 4B). To assess reference memory, a probe trial was conducted 24 h after the last acquisition period. Figure 4C shows the percent time in the target quadrant and an increased time spent in quadrants other than the target quadrant is indicative of impaired spatial learning, as observed in the ethanol group (Figure 4C, $p < 0.01$). Upon treatment with 5 mg/kg **P8** and **P9**, the animals displayed significantly improved spatial memory and learning (Figure 4C, $p < 0.05$). Additionally, a Y-maze test (Figure 4D) was conducted to assess the

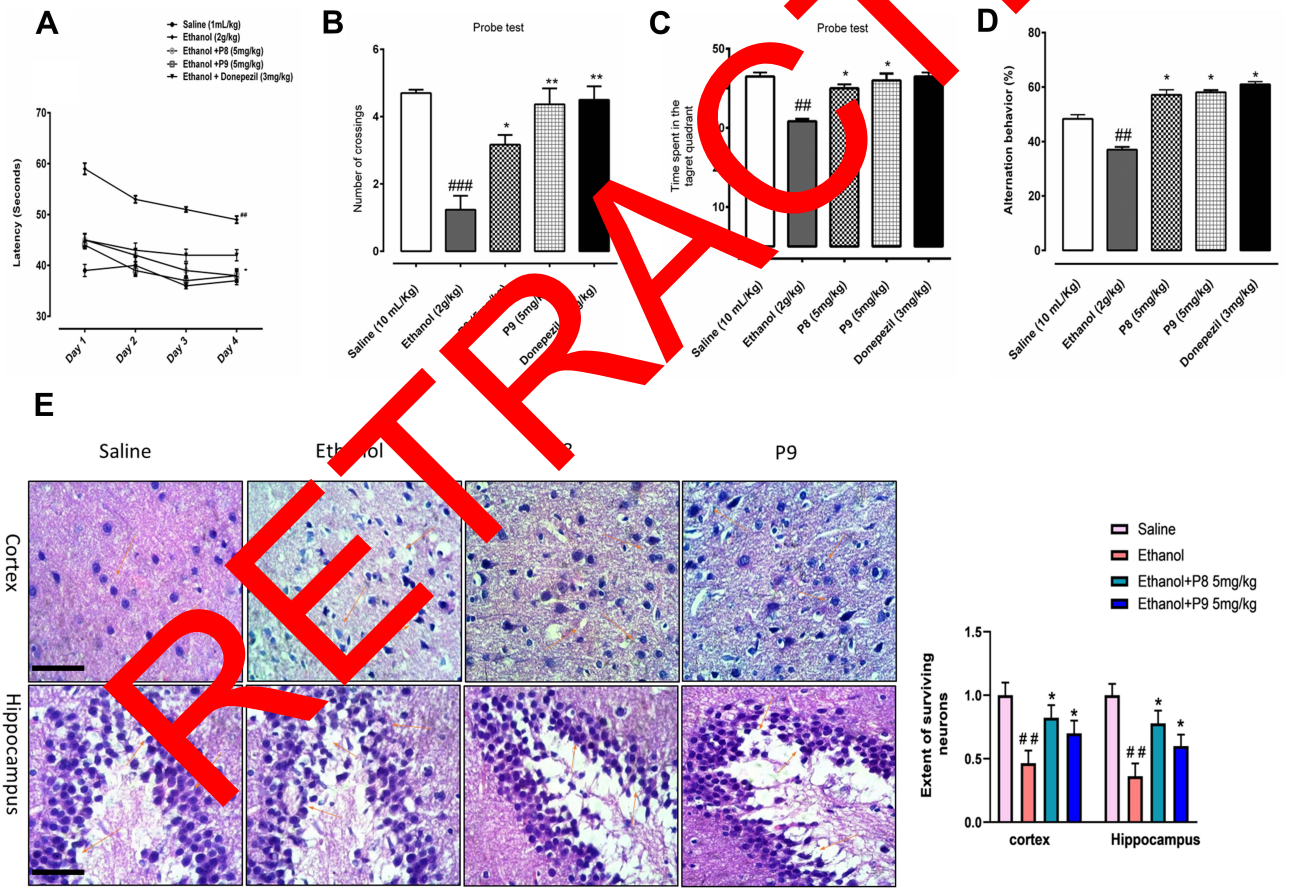

Figure 4 Compounds P8 and P9 improved the memory function of the ethanol-treated rats. For the behavioral analyses, the MWM and Y-maze tests were used to investigate and evaluate the memory functions of the control, ethanol, ethanol + compound P8, ethanol + compound P9, and ethanol + donepezil. (**A**) Average escape latency time for experimental rats to reach the hidden probe from day 1 to day 4. (**B**) The average number of platform crossings of experimental rats during the probe test of the MWM test. (**C**) Average time spent by experimental animals in the target quadrant on day 5. (**D**) Spontaneous alteration behavior % of the animals during the Y-maze test. Histograms indicate the mean ± SEM for the rats (n = 16/group). (**E**) Representative immunohistochemical images of H and E and the quantified histogram of the survival neuron reactivity and integrated density in the cortex and hippocampus region of adult cortex. Symbols $^{\#\#}$Or **Shows significant difference $p < 0.01$, $^{\#\#\#}$Shows significant difference $p < 0.001$, while *Shows significant difference $p < 0.05$. *Sign shows significant difference from disease group (ethanol-treated). Values are given as mean ± SEM; Statistical analysis by one-way ANOVA. Scale bar 50 μm, magnification 40×, (n=8/group).

percentage of spontaneous alternation behavior in rats. Ethanol-treated animals demonstrated a significant behavior deficit as shown by the fewer percentage of alternation in the Y-maze (Figure 4D, $p < 0.01$). On the other hand, synthetic derivatives significantly enhance the percentage of alternation compared to the ethanol-alone injected group, and this effect was not due to locomotor effects, as shown in Figure 4D. Here, the thiazolidine derivatives reduced the ethanol-prolonged escape latency time, which indicated improvement in ethanol-induced spatial memory impairment as shown previously. To further validate our hypothesis, we examined morphological changes in the cortical and hippocampal regions using H & E staining. The saline group showed round, well-demarcated intact cells without nuclear condensation or distortion with a basophilic cytoplasm (Figure 4E). The ethanol-treated group showed significant histopathological alterations, including altered neuronal shape and size, as well as other atypical features, including swollen, flattened, atrophied, and karyolitic neurons with pyknotic nuclei (Figure 4E). Examination of cortical and hippocampal areas validated that our newly synthesized drugs significantly ameliorated these morphological dam[illegible]s indicated by an increase in the number of intact neurons and cell count (Figure 4E, cortex: $*p < 0.05$ and [illegible]G: $*p < 0.$[illegible]).

Effect of Thiazolidine Derivatives (P8 & P9) on Oxidative Enzymes

In the ethanol group, a significant reduction in GST, GSH, and catalase levels (F[illegible]re 5A[illegible], $p < 0.01$) was demonstrated associated with a significant elevation in the activity of LPO (Figure 5D, [illegible] < 0.0[illegible] **P8** and [illegible] reversed the effect of

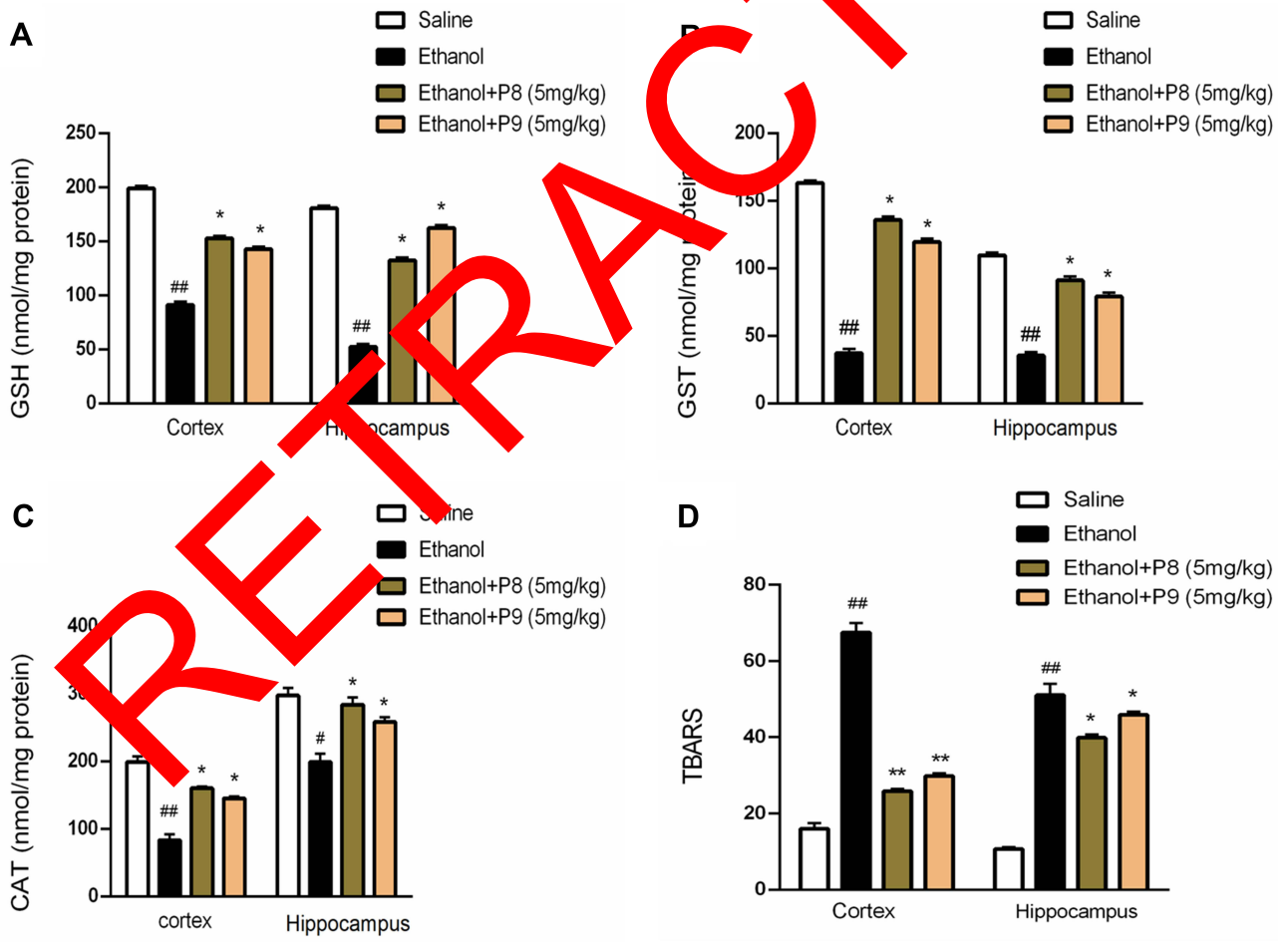

Figure 5 Pretreatment with compounds P8 and P9 significantly improved the GSH (**A**), GST (**B**), and CAT (**C**) antioxidant enzymes in treated groups while the TBARS levels (**D**) were reduced. Symbols ##Or **Shows significant difference $p < 0.01$, while #Or *Shows significant difference $p < 0.05$. #Shows significant difference relative to control while *Shows significant difference from disease group (ethanol-treated). All data were analyzed by one-way ANOVA followed by a post hoc Bonferroni multiple comparison test. Data were presented as means ± SEM.

Abbreviations: GST, glutathione S-transferase; GSH, glutathione; TBRAS, thiobarbituric acid reactive substances.

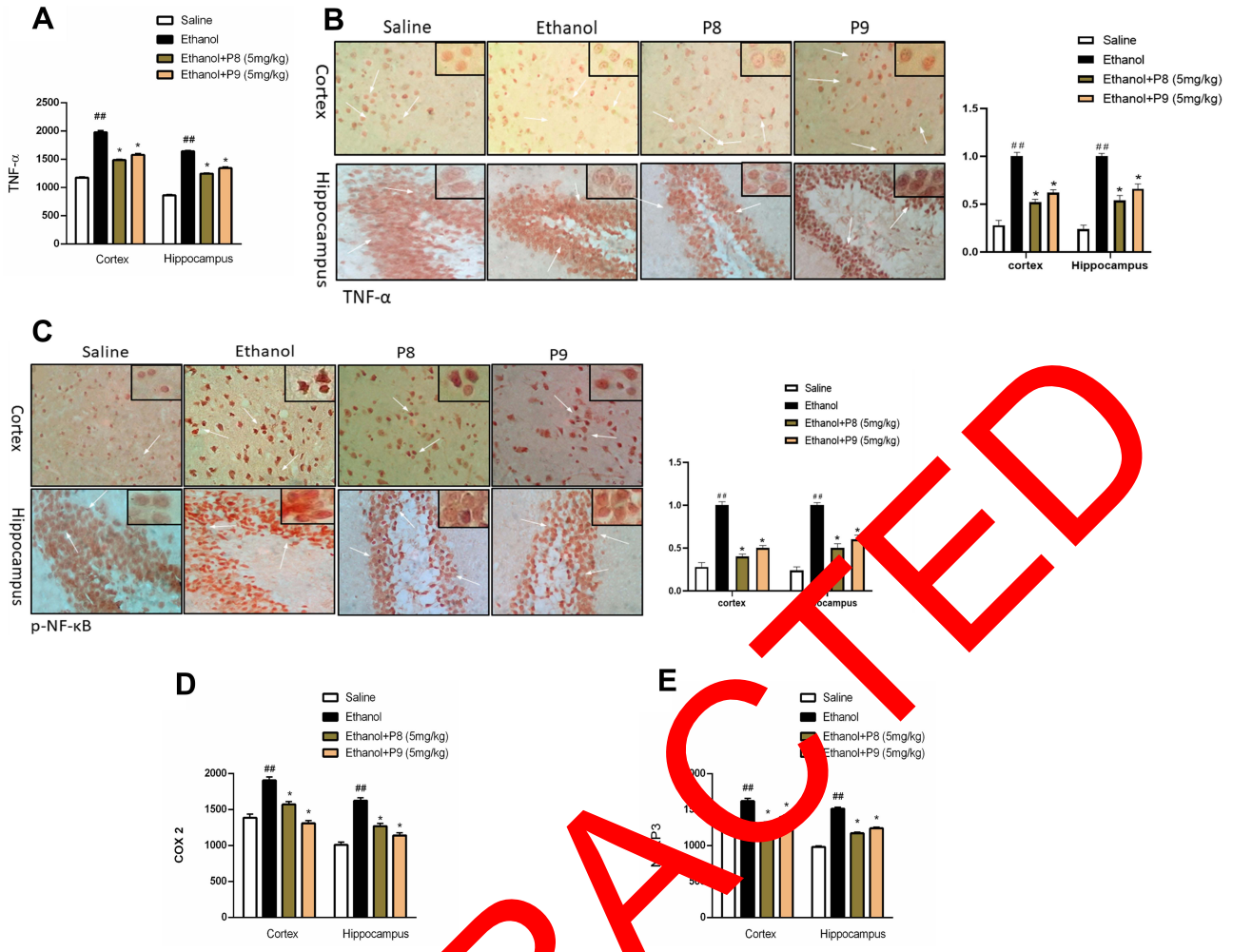

Figure 6 Thiazolidine derivatives attenuated inflammatory m[illegible]tors i[illegible]ted animals. (**A**) TNF-α protein expression as quantified by ELISA with (n=8/group). (**B**) Immunohistochemistry results for TNF-α in the c[illegible]ical an[illegible]campal tissues with (n=8/group). TNF-α exhibited cytoplasmic localization in the treated tissue. (**C**) p-NF-KB protein expression as quantified by immu[illegible]istochemistr[illegible]th (n=8/group). (**D**) ELISA analysis of COX-2 (**E**) NLRP3 from cortical and hippocampal tissues with (n=8/group). All data were expressed as Mean [illegible] Symbols ###Sho[illegible]ignificant difference $p < 0.01$, while *Shows significant difference $p < 0.05$. The symbol *Indicates a significant difference relative to the ethanol group.

ethanol and normalize[illegible]he anti[illegible]idant enzyme levels of GSH ($p < 0.05$), GST ($p < 0.05$), and catalase ($p < 0.05$), while reducing the elevated le[illegible] LPO as[illegible]hown in ($p < 0.05$).

Effect of P8 an[illegible] P9 on Ethanol-Induced Inflammatory Mediators

Inflammatory [illegible]iators play a significant role in memory impairment; we sought to investigate whether **P8** and **P9** will influence neuroi[illegible]mmation. As a result, we used ELISA and immunohistochemistry to study the expression of TNF-α, NLRP3, COX-2, an[illegible]p-NF-κB, in the cortex and hippocampus. Ethanol provoked the expression of these inflammatory markers and a higher expression was demonstrated in the ethanol group in comparison to the saline group (Figure 6, $p < 0.01$). **P8** and **P9** treatment resulted in a substantial decrease of these markers in the cortex and hippocampus compared to the ethanol population (Figure 6, $p < 0.05$).

Discussion

Thiazolidine core has been reported in many pharmaceutical formulations in recent years due to its high pharmacological activities.[12–19] More interestingly, these molecules have a diverse applications and are marketed as potential candidate drugs against various disorders and are recently reviewed by Sahiba et al.[12] Keeping in view the pharmacological

importance, including its safety records and BBB penetration, we have synthesized a new series of thiazolidine-4-carboxylic acid derivatives that can target multiple steps of the inflammatory cascade. For this purpose, a multi-reactions scheme was adopted and ten new thiazolidine-4-carboxylic acid derivatives **(P1-P10)** were synthesized and preliminary screened for in vitro antioxidant activity. The substitutions of nitro (**P6**) and methoxy (**P7**) groups on the benzene ring lead to an increase in antioxidant activity. Moreover, the introduction of halogens on phenyl moiety (**P2-P5 and P10**) further improved the antioxidant potential. However, the activity was sharply increased after the introduction of the -OH group (**P8, P9**) on the benzene ring. The reason for the significant antioxidant activity was the presence of phenolic moiety in the structures of compounds **P8** and **P9**. Phenolic compounds possess strong antioxidant properties and many natural compounds with phenolic moiety consistently showed favorable biological activities.[62,63] Moreover, the usage of compounds containing phenol structural moiety has been extensively studied in the treatment of neurodegenerative diseases such as Alzheimer's disease, Parkinson's disease, and Huntington´s disease.[62,63] Therefore, compounds (**P8** and **P9**) were selected for further in vivo studies. We have synthesized thiazolidine-4-carboxylic acid derivatives and demonstrated its neuroprotective role in an ethanol-induced neurodegenerative model. The synthesized analogs downregulated the complex cascades of oxidative stress-induced inflammation. Most neurodegenerative disorders are characterized by complicated pathophysiology owing to the complex brain nature and for this reason, several drugs have been tested in animal experimental models, yet not a single drug qualified the clinical testing.[64]

Here, we have targeted the main pathological hallmarks of neurodegenerative diseases, oxidative stress, and neuroinflammation.[65] Consistent human data reiterated the generation of free radicals via ethanol consumption,[43,44] and such amassing precipitated cognitive impairment due to narrow anti-oxidants in the brain.[66] Ethanol has a high propensity for ROS generation and this is further validated by an elevated level of LPO along with a reduced glutathione level and which is consistent with previous findings.[36] According to the previously reported study, thiazolidine derivatives have tremendous potential to attenuate memory impairment and neuroinflammation.[67] Many published reports are evidencing the relationship between oxidative stress and stimulation of inflammatory cascades.[68–70] Increased oxidative stress and lower levels of antioxidant enzymes may have critical effects on brain tissues.[71,72] Thus, successful therapeutic approaches should aim at controlling the neuroinflammation as well as attenuating oxidative stress via stimulating the anti-oxidant enzymes. Several studies reported the antioxidant and anti-inflammatory activities of thiazolidine derivatives.[14,15,20–24] GSH, GST, and catalase play a super role in the suppression of free radicals[73] Numerous thiazolidine derivatives have been reported as antioxidants through activating GSH and inhibiting LPO.[24,74] Pretreatment using selected thiazolidine-4-carboxylic acid derivatives **(P8 and P9)** significantly increased the levels of GSH, GST, and catalase and reduced the LPO in brain homogenates and thus helping to combat the brain against ethanol-induced oxidative stress.

Neuroinflammation triggers the release of ROS, which is responsible for oxidative stress, and which aids in exacerbating the pathogenesis of neurodegenerative diseases including memory impairment, cognitive deficits, and other behavioral abnormalities.[75] Activation of the NLRP3 inflammasome has been linked to the development of several diseases and inflammatory disorders, particularly those that are age-related, such as Alzheimer's disease, and type II diabetes (T2D).[76,77] The release of reactive oxygen species (ROS) and pro-inflammatory mediators such as interleukin-1 (IL-1β) and tumor necrosis factor-alpha (TNF-α) leads to cellular damage and lipid peroxidation.[78] In a neurodegenerative brain, TNF-α induced NF-κB play a central role in the regulation of inflammation following different transcriptional and transduction pathways.[79] According to the published literature, the activation of NF-κB inflammatory pathways is directly related to the attachment of TNF-α to its respective receptor.[80] Inhibition of TNF-α helps to alleviate not only inflammation but also cognitive deficits.[81] In the present study, marked elevation of TNF-α was observed in neurodegenerative brains. While, pre-administering thiazolidine derivatives **(P8 and P9)** attenuated the overexpression of TNF-α, NF-κB, NLRP3, and COX-2 in ethanol-treated rat brain and accordingly reversed the stimulation of the NF-κB and NLRP3 signaling pathways. Moreover, molecular docking studies against several targets involved in neuroinflammation such as NF-κB, NLRP3, TLR4, and COX-2 also revealed neuroprotective effects of synthesized compounds. This study advises these analogs especially **P8 and P9** can reduce neuronal damage by downregulating the overexpression of proinflammatory cytokines and further by modulating the p-NF-κB and NLRP3 pathway.

Conclusion

Ethanol-exposed neuronal damage activates numerous pro-inflammatory cytokines including TNF-α, NF-κB, NLRP3 and COX-2, and has a dominating association with oxidative stress. These newly designed novel thiazolidine-4-carboxylic acid derivatives **(P8 and P9)** reversed the ethanol-exposed oxidative stress and inflammatory cascade possibly by reducing the ROS/NF-κB/NLRP3/TNF-α/COX-2 cascade, which ultimately leads to their neuroprotective role against neurodegenerative diseases.

Author Contributions

All authors made substantial contributions to conception and design, acquisition of data, or analysis and interpretation of data; took part in drafting the article or revising it critically for important intellectual content; agreed to submit to the current journal; gave final approval of the version to be published, and agree to be accountable for all aspects of the work.

Funding

This study was completed without any financial support.

Disclosure

The authors report no conflicts of interest in this work.

References

1. Heemels MT. Neurodegenerative diseases. *Nature*. 2016;539(7628):179–180. doi:10.1038/539179a
2. Durães F, Pinto M, Sousa E. Old drugs as new treatments for neurodegenerative diseases. *Pharmaceuticals*. 2018;11(2):44. doi:10.3390/ph11020044
3. Di Stefano A, Reale M. Neurodegenerative disorders: synthesis, delivery strategies and biological evaluation of new therapeutic agents. *Cent Nerv Syst Agents Med Chem*. 2017;17(2):89. doi:10.2174/1871524917666170712214058
4. Brettschneider J, Del Tredici K, Lee VMY, Trojanowski JQ. Spreading of pathology in neurodegenerative diseases: a focus on human studies. *Nat Rev Neurosci*. 2015;16(2):109–120. doi:10.1038/nrn3887
5. Soto C, Pritzkow S. Protein misfolding, aggregation, and conformational strains in neurodegenerative diseases. *Nat Neurosci*. 2018;21(10):1332–1340. doi:10.1038/s41593-018-0235-9
6. Gitler AD, Dhillon P, Shorter J. Neurodegenerative disease: models, mechanisms, and a new hope. *Dis Model Mech*. 2017;10:499–502. doi:10.1242/dmm.030205
7. Hickman SE, Allison EK, El Khoury J. Microglial dysfunction and defective β-amyloid clearance pathways in aging Alzheimer's disease mice. *J Neurosci*. 2008;28(33):8354–8360. doi:10.1523/JNEUROSCI.0616-08.2008
8. Vuong T, Mallet JF, Ouzounova M, et al. Role of a polyphenol-enriched preparation on chemoprevention of mammary carcinoma through cancer stem cells and inflammatory pathways modulation. *J Transl Med*. 2016;14(1):1–12. doi:10.1186/s12967-016-0770-7
9. Mott M, Koroshetz W. Bridging the gap in neurotherapeutic discovery and development: the role of the National Institute of Neurological Disorders and Stroke in translational neuroscience. *Neurotherapeutics*. 2015;12(3):651–654. doi:10.1007/s13311-015-0366-6
10. Zhang H, Zhang J, Qu, et al. Design, synthesis, and biological evaluation of novel thiazolidinone-containing quinoxaline-1, 4-di-N-oxides as antimycobacterial and anti agents. *Front Chem*. 2020;8:598. doi:10.3389/fchem.2020.00598
11. Lu Y, Li CM, Wa et al. Discovery of substituted methoxybenzoyl-aryl-thiazole as Novel Anticancer Agents: synthesis, biological evaluation, and structure activity relationship. *Med Chem*. 2009;52(6):1701–1711. doi:10.1021/jm801449a
12. Sahiba N, thiya A, ni J, Agarwal DK, Agarwal S. Saturated five-membered thiazolidines and their derivatives: from synthesis to biological application. *Top C* 020;378(2):1–90.
13. Makwana HR, ani AH, Brief Review A. Article: thiazolidines derivatives and their pharmacological activities. *J Appl Chem*. 2017;10:76–84.
14. Apostolidis I, Li K, Geronikaki A, et al. Synthesis and biological evaluation of some 5-arylidene-2-(1, 3-thiazol-2-ylimino)-1, 3-thiazolidin-4-ones as dual anti- ammatory/antimicrobial agents. *Bioorg Med Chem*. 2013;21(2):532–539. doi:10.1016/j.bmc.2012.10.046
15. Abdellatif KR, Abdelgawad MA, Elshemy HA, Alsayed SS. Design, synthesis and biological screening of new 4-thiazolidinone derivatives with promising COX-2 selectivity, anti-inflammatory activity and gastric safety profile. *Bioorg Chem*. 2016;64:1–12. doi:10.1016/j.bioorg.2015.11.001
16. Liu Y, Jing F, Xu Y, et al. Design, synthesis and biological activity of thiazolidine-4-carboxylic acid derivatives as novel influenza neuraminidase inhibitors. *Bioorg Med Chem*. 2011;19(7):2342–2348. doi:10.1016/j.bmc.2011.02.019
17. Zhang Q, Zhou H, Zhai S, Yan B. Natural product-inspired synthesis of thiazolidine and thiazolidinone compounds and their anticancer activities. *Curr Pharm Des*. 2010;16(16):1826–1842. doi:10.2174/138161210791208983
18. Jagtap RM, Thorat SH, Gonnade RG, Khan AA, Pardeshi SK. X-ray crystal structures and anti-breast cancer property of 3-tert-butoxycarbonyl -2-arylthiazolidine-4-carboxylic acids. *New J Chem*. 2018;42(2):1078–1086. doi:10.1039/C7NJ02961F
19. Das Neves AM, Berwaldt GA, Avila CT, et al. Synthesis of thiazolidin-4-ones and thiazinan-4-ones from 1-(2-aminoethyl) pyrrolidine as acetylcholinesterase inhibitors. *J Enzyme Inhib Med Chem*. 2020;35(1):31–41. doi:10.1080/14756366.2019.1680659
20. Marc G, Stana A, Oniga SD, Pîrnău A, Vlase L, Oniga O. New phenolic derivatives of thiazolidine-2, 4-dione with antioxidant and antiradical properties: synthesis, characterization, in vitro evaluation, and quantum studies. *Molecules*. 2019;24(11):2060. doi:10.3390/molecules24112060

21. Lupaşcu F, Dragostin OM, Apotrosoaei M, et al. Synthesis and evaluation of antioxidant activity of some new benzylidene-thiazolidine-xanthine derivatives. *Rev Med Chir Soc Med Nat Iasi*. 2013;117:244–249.
22. Ham YH, Jason Chan KK, Chan W. Thioproline serves as an efficient antioxidant protecting human cells from oxidative stress and improves cell viability. *Chem Res Toxicol*. 2020;33(7):1815–1821. doi:10.1021/acs.chemrestox.0c00055
23. Jagtap RM, Pardeshi SK. Antioxidant activity screening of a series of synthesized 2-aryl thiazolidine-4-carboxylic acids. *Der Pharm Lett*. 2014;6 (3):137–145.
24. Yan Y, Wan-Shun L, Bao-Qin H, Hai-Zhou S. Antioxidative properties of a newly synthesized 2-glucosamine-thiazolidine-4 (R)-carboxylic acid (GlcNH2Cys) in mice. *Nutr Res*. 2006;26(7):369–377. doi:10.1016/j.nutres.2006.06.014
25. Gomathy S, Singh G, Gowramma B, Antony AS, Elango K. Synthesis and anti-Parkinson's screening of some novel 2-(naphthalen-1-yl)-N-[2-substituted (4-oxothiazolidin-3-yl)] acetamide derivatives. *Int J Health Allied Sci*. 2012;1(4):244–248. doi:10.4103/2278-344X.107871
26. Wang Y, Zhao W, Li G, et al. Neuroprotective effect and mechanism of thiazolidinedione on dopaminergic neurons in vivo and in vitro in Parkinson's disease. *PPAR Res*. 2017;2017:1–12. doi:10.1155/2017/4089214
27. Sadashiva CT, Chandra JNS, Kavitha CV, Thimmegowda A, Subhash MN, Rangappa KS. Synthesis and pharmacological evaluation of novel N-alkyl/aryl substituted thiazolidinone arecoline analogues as muscarinic receptor 1 agonist in Alzheimer's dementia models. *Eur J Med Chem*. 2009;44(12):4848–4854. doi:10.1016/j.ejmech.2009.07.026
28. Zhao L, Huang W, Liu H, et al. FK506-binding protein ligands: structure-based design, synthesis, and neurotrophic/neuroprotective properties of substituted 5, 5-dimethyl-2-(4-thiazolidine) carboxylates. *J Med Chem*. 2006;49(14):4059–4071. doi:10.1021/[illegible]0502384
29. Gandini A, Bartolini M, Tedesco D, et al. Tau-centric multitarget approach for Alzheimer's disease: development of first-in-class dual glycogen synthase kinase 3β and tau-aggregation inhibitors. *J Med Chem*. 2018;61(17):7640–7656. doi:10.1021/[illegible]s.jmedchem.8b00610
30. Kumar B, Mantha AK, Kumar V, Kumar V. Recent developments on the structure–activity relationship studies of MAO inhibitors and their role in different neurological disorders. *RSC Adv*. 2016;6(48):42660–42683. doi:10.1039/C6RA00302H
31. Zhang YF, Zou XL, Jun WU, Yu XQ, Yang X. Rosiglitazone, a peroxisome proliferator-activated receptor (PPAR)-γ agonist, attenuates inflammation via NF-κB inhibition in lipopolysaccharide-induced peritonitis. *Inflammation*. 2015;38(6):2105–2[illegible]. doi:[illegible]7/s10753-015-0193-2
32. Kaplan J, Nowell M, Chima R, Zingarelli B. Pioglitazone reduces inflammation through inhibition of NF-κB in polymicrobial sepsis. *Innate Immun*. 2014;20(5):519–528. doi:10.1177/1753425913501565
33. Saito M, Chakraborty G, Hui M, Masiello K, Saito M. Ethanol-induced neurodegeneration and glial activation in the developing brain. *Brain Sci*. 2016;6(3):31. doi:10.3390/brainsci6030031
34. Al Kury LT, Zeb A, Abidin ZU, et al. Neuroprotective effects of melatonin and celecoxib against ethanol-induced neurodegeneration: a computational and pharmacological approach. *Drug Des Devel Ther*. 2019;13:2715. doi:10.2147/DDDT.S207310
35. Ali T, Rehman SU, Shah FA, Kim MO. Acute dose of melatonin via Nrf2 dependently prevents acute ethanol-induced neurotoxicity in the developing rodent brain. *J Neuroinflammation*. 2018;15(1):1–19. doi:10.[illegible]86/s12974-018-[illegible]157-x
36. Imran M, Al Kury LT, Nadeem H, et al. Benzimidazole containing acetamide derivatives attenuate neuroinflammation and oxidative stress in ethanol-induced neurodegeneration. *Biomolecules*. 2020;10([illegible]. doi:10.339[illegible]3010108
37. Yin J, Valin KL, Dixon ML, Leavenworth JW. The role of microglia and macrophages in CNS homeostasis, autoimmunity, and cancer. *J Immunol Res*. 2017;2017:1–12. doi:10.1155/2017/5150678
38. Rao JS, Rapoport SI, Kim HW. Altered neuroinflammatory, arachidonic acid cascade and synaptic markers in postmortem Alzheimer's disease brain. *Transl Psychiatry*. 2011;1(8):e31–e31. doi:10.10[illegible]p.2011.[illegible]7
39. Dean B, Tawadros N, Scarr E, Gibbons AS. Regionally specific changes in levels of tumour necrosis factor in the dorsolateral prefrontal cortex obtained postmortem from subjects with major depressive disorder. *J Affect Disord*. 2010;120(1–3):245–248. doi:10.1016/j.jad.2009.04.027
40. Menachem-Zidon OB, Goshen I, Kreisel T, et al. Intrahippocampal transplantation of transgenic neural precursor cells overexpressing interleukin-1 receptor antagonist blocks chronic isolation-induced impairment in memory and neurogenesis. *Neuropsychopharmacology*. 2008;33(9):2251–2262. doi:10.1038/sj.npp.1301606
41. Goshen I, Kreisel T, Ben-Menachem-Zidon O, et al. Brain interleukin-1 mediates chronic stress-induced depression in mice via adrenocortical activation and hippocampal neurogenesis suppression. *Mol Psychiatry*. 2008;13(7):717–728. doi:10.1038/sj.mp.4002055
42. Yirmiya R, Pollak Y, Morag M, et al. Illness, cytokines, and depression. *Ann N Y Acad Sci*. 2000;917(1):478–487. doi:10.1111/j.1749-6632.2000.tb05412.x
43. Eckardt MJ, File SE, Gessa GL, et al. Effects of moderate alcohol consumption on the central nervous system. *Alcohol Clin Exp Res*. 1998;22 (5):998–1040. doi:[illegible]1111/j.[illegible]50-0277.1998.tb03695.x
44. Reddy VD, Padmavathi P, Kavitha G, Saradamma B, Varadacharyulu N. Alcohol-induced oxidative/nitrosative stress alters brain mitochondrial membrane properties. *Mol Cell Biochem*. 2013;375(1):39–47. doi:10.1007/s11010-012-1526-1
45. Vallés S, Blanco AM, Pascual M, Guerri C. Chronic ethanol treatment enhances inflammatory mediators and cell death in the brain and in astrocytes. *Brain Pathol*. 2004;14(4):365–371. doi:10.1111/j.1750-3639.2004.tb00079.x
46. Franchi L, Eigenbrod T, Muñoz-Planillo R, Nunez G. The inflammasome: a caspase-1-activation platform that regulates immune responses and disease pathogenesis. *Nat Immunol*. 2009;10(3):241–247. doi:10.1038/ni.1703
47. Gong Z, Pan J, Shen Q, Li M, Peng Y. Mitochondrial dysfunction induces NLRP3 inflammasome activation during cerebral ischemia/reperfusion injury. *J Neuroinflammation*. 2018;15(1):1–17. doi:10.1186/s12974-018-1282-6
48. Toma C, Higa N, Koizumi Y, et al. Pathogenic Vibrio activate NLRP3 inflammasome via cytotoxins and TLR/nucleotide-binding oligomerization domain-mediated NF-κB signaling. *J Immunol*. 2010;184(9):5287–5297. doi:10.4049/jimmunol.0903536
49. Qiao Y, Wang P, Qi J, Zhang L, Gao C. TLR-induced NF-κB activation regulates NLRP3 expression in murine macrophages. *FEBS Lett*. 2012;586 (7):1022–1026. doi:10.1016/j.febslet.2012.02.045
50. Muñoz-Planillo R, Kuffa P, Martínez-Colón G, Smith BL, Rajendiran TM, Núñez G. K+ efflux is the common trigger of NLRP3 inflammasome activation by bacterial toxins and particulate matter. *Immunity*. 2013;38(6):1142–1153. doi:10.1016/j.immuni.2013.05.016
51. Jiang H, Yan Y, Jiang W, Zhou R. NLRP3 inflammasome: activation, regulation, and role in diseases. *Sci Sin*. 2017;47(1):125–131.
52. Laudien R, Yoshida I, Nagamura T. Synthesis and photophysical properties of porphyrins containing viologen units for ultrafast molecular photonics. *J Chem Soc Perkin Trans*. 2002;2(10):1772–1777. doi:10.1039/B202991J
53. Abbas Q, Ashraf Z, Hassan M, et al. Development of highly potent melanogenesis inhibitor by in vitro, in vivo and computational studies. *Drug Des Devel Ther*. 2017;11:2029. doi:10.2147/DDDT.S137550

54. Shoaib M, Shah A, Wadood S, et al. In Vitro Enzyme Inhibition Potentials and Antioxidant Activity of Synthetic Flavone Derivatives. *J Chem*. 2015;2015:1–7. doi:10.1155/2015/516878
55. Ali T, Badshah H, Kim TH, Kim MO. Melatonin attenuates D-galactose-induced memory impairment, neuroinflammation and neurodegeneration via RAGE/NF-KB/JNK signaling pathway in aging mouse model. *J Pineal Res*. 2015;58(1):71–85. doi:10.1111/jpi.12194
56. Khan A, Shal B, Naveed M, et al. Matrine ameliorates anxiety and depression-like behaviour by targeting hyperammonemia-induced neuroinflammation and oxidative stress in CCl4 model of liver injury. *Neurotoxicology*. 2019;72:38–50. doi:10.1016/j.neuro.2019.02.002
57. Kurban S, Deniz NG, Sayil C, et al. Synthesis, antimicrobial properties, and inhibition of catalase activity of 1, 4-naphtho-and benzoquinone derivatives containing N-, S-, O-substituted. *Heteroat Chem*. 2019;2019:1–12. doi:10.1155/2019/1658417
58. Shah FA, Park DJ, Koh PO. Identification of proteins differentially expressed by quercetin treatment in a middle cerebral artery occlusion model: a proteomics approach. *Neurochem Res*. 2018;43(8):1608–1623. doi:10.1007/s11064-018-2576-x
59. Volkamer A, Kuhn D, Grombacher T, Rippmann F, Rarey M. Combining global and local measures for structure-based druggability predictions. *J Chem Inf Model*. 2012;52(2):360–372. doi:10.1021/ci200454v
60. O'Boyle NM, Banck M, James CA, Morley C, Vandermeersch T, Hutchison GR. Open babel: an open chemical toolbox. *J Cheminformatics*. 2011;3(1):1–14.
61. Trott O, Olson AJ. AutoDock Vina: improving the speed and accuracy of docking with a new scoring function, efficient optimization, and multithreading. *J Comput Chem*. 2010;31(2):455–461. doi:10.1002/jcc.21334
62. Neha K, Haider MR, Pathak A, Yar MS. Medicinal prospects of antioxidants: a review. *Eur J Med Chem*. 2019;178:687–704. doi:10.1016/j.ejmech.2019.06.010
63. Pisoschi AM, Pop A. The role of antioxidants in the chemistry of oxidative stress: a review. *Eur J Med Chem*. 2015;97:55–74. doi:10.1016/j.ejmech.2015.04.040
64. Van der Schyf CJ. The use of multi-target drugs in the treatment of neurodegenerative diseases. *Expert Rev Clin Pharmacol*. 2011;4(3):293–298. doi:10.1586/ecp.11.13
65. Lindqvist D, Dhabhar FS, James SJ, et al. Oxidative stress, inflammation and treatment response in major depression. *Psychoneuroendocrinology*. 2017;76:197–205. doi:10.1016/j.psyneuen.2016.11.031
66. Salim S. Oxidative stress and the central nervous system. *J Pharmacol Exp Ther*. 2017;360(1):201–205. doi:10.1124/jpet.116.237503
67. Wang XK, Sun T, Li YJ, et al. A novel thiazolidinediones ATZD2 rescues memory deficit in a rat model of type 2 diabetes through antioxidant and antiinflammation. *Oncotarget*. 2017;8(64):107409. doi:10.18632/oncotarget.22467
68. Ganguly U, Kaur U, Chakrabarti SS, et al. Oxidative stress, neuroinflammation, and NADPH oxidase: implications in the pathogenesis and treatment of Alzheimer's disease. *Oxid Med Cell Longev*. 2021;2021:1–19. doi:10.1155/2021/7086512
69. He J, Zhu G, Wang G, Zhang F. Oxidative stress and neuroinflammation potentiate each other to promote progression of dopamine neurodegeneration. *Oxid Med Cell Longev*. 2020;2020:1–12. doi:10.1155/2020/6137521
70. Hassanzadeh K, Rahimmi A. Oxidative stress and neuroinflammation in the story of Parkinson's disease: could targeting these pathways write a good ending? *J Cell Physiol*. 2019;234(1):23–32. doi:10.1002/jcp.26865
71. Gu F, Zhu M, Shi J, Hu Y, Zhao Z. Enhanced oxidative stress is an early event during development of Alzheimer-like pathologies in presenilin conditional knock-out mice. *Neurosci Lett*. 2008;440(1):44–48. doi:10.1016/j.neulet.2008.05.050
72. Markesbery WR. Oxidative stress hypothesis in Alzheimer's disease. *Free Radic Biol Med*. 1997;23(1):134–147. doi:10.1016/S0891-5849(96)00629-6
73. Lee KH, Cha M, Lee BH. Neuroprotective effect of antioxidants in the brain. *Int J Mol Sci*. 2020;21(19):7152. doi:10.3390/ijms21197152
74. Bayram FEÖ, Sipahi H, Acar ET, Ulugöl RK, Bu[illegible]n K, Ak[illegible]n H. The cysteine releasing pattern of some antioxidant thiazolidine-4-carboxylic acids. *Eur J Med Chem*. 2016;114:337–344. doi:10.1016/j.ejmech.2016.03.019
75. Pascual M, Blanco AM, Cauli O, Miñarro J, Guerri C. Intermittent ethanol exposure induces inflammatory brain damage and causes long-term behavioural alterations in adolescent rats. *Eur J Neurosci*. 2007;25(2):541–550. doi:10.1111/j.1460-9568.2006.05298.x
76. Halle A, Hornung V, Petzold GC, et al. The NALP3 inflammasome is involved in the innate immune response to amyloid-β. *Nat Immunol*. 2008;9(8):857–865. doi:10.1038/ni.1636
77. Lee HM, Kim JJ, Kim HJ, Shong M, Ku BJ, Jo EK. Upregulated NLRP3 inflammasome activation in patients with type 2 diabetes. *Diabetes*. 2013;62(1):194–204. doi:10.2337/db12-0420
78. Mittal M, Siddiqui MR, Tran K, Reddy SP, Malik AB. Reactive oxygen species in inflammation and tissue injury. *Antioxid Redox Signal*. 2014;20(7):1126–1167. doi:10.1089/ars.2012.5149
79. Samuelsson M, Fisher L, Lefvert K. β-Amyloid and interleukin-1β induce persistent NF-κB activation in rat primary glial cells. *Int J Mol Med*. 2005;16(3):449–
80. Shah FA, Ku[illegible]LA, Li[illegible] et al. Pe[illegible]da[illegible] attenuates neuronal loss via reducing neuroinflammation and oxidative stress in rat MCAO models. *Front Pharmacol*. 2019;10:6[illegible]. doi:10.3389/fphar.2019.00663
81. Bortolato B, Carvalho AF, Soczynska J, et al. The involvement of TNF-α in cognitive dysfunction associated with major depressive disorder: an opportunity for domain specific treatments. *Curr Neuropharmacol*. 2015;13(5):558–576. doi:10.2174/1570159X13666150630171433